Phys. Status Solidi A **210**, No. 12, 2583–2587 (2013) / **DOI** 10.1002/pssa.201330119

physica status solidi a
www.pss-a.com
applications and materials science

Tandem organic light-emitting diodes with an effective nondoped charge-generation unit

Bo Jiao[1,2], Zhaoxin Wu*[,1,2], Zhiyuan Yang[3], and Xun Hou[1]

[1] Key Laboratory of Photonics Technology for Information, School of Electronic and Information Engineering, Xi'an Jiaotong University, Xi'an, Shannxi 710049, P.R. China
[2] Key Laboratory for Physical Electronics and Devices of the Ministry of Education, School of Electronic and Information Engineering, Xi'an Jiaotong University, Xi'an, Shannxi 710049, P.R. China
[3] School of Information Science and Technology, Northwest University, Xi'an, Shannxi 710069, P.R. China

Received 10 July 2013, revised 7 August 2013, accepted 12 August 2013
Published online 20 September 2013

Keywords charge generation, molybdenum aluminum trioxide, tandem organic light-emitting diodes, tris(8-hydroxyquinoline)

* Corresponding author: e-mail zhaoxinwu@mail.xjtu.edu.cn, Phone +86-29-82664867, Fax: +86-29-82664867

An undoped charge-generation unit (CGU) with the structure of lithium fluoride (LiF)/aluminum/molybdenum trioxide (MoO_3) was demonstrated in tandem organic light-emitting diodes (OLEDs). Tandem OLEDs with two identical emissive units consisting of 4,4′-bis-(1-naphthyl-*N*-phenylamino)-biphenyl (NPB)/tris(8-hydroxyquinoline) aluminum (Alq_3) exhibited superior performance over a corresponding single-unit device. Under a driving current of 650 A m^{-2}, the current efficiency of the tandem OLEDs was about 6.95 cd A^{-1}, almost double that of the single-unit OLEDs. The operational stability of the tandem OLEDs was also enhanced compared with that of the single-unit OLEDs. It was demonstrated that the MoO_3 plays a critical role of charge generation in this undoped CGU. The LiF/Al layers were used to enhance the electron injection from MoO_3 layer to the adjacent Alq_3 layer. Furthermore, fabrication of this CGU involves no sputtering or doping process, which can render tandem OLEDs processing more feasible.

1 Introduction Tandem organic light-emitting diodes (OLEDs) have received considerable attention for their advantages of enhanced current efficiency and luminance at low current density, as well as the prolonged lifetime as compared to conventional single-unit OLEDs [1–19]. The typical structure of tandem OLEDs consists of two or multiple electroluminescence (EL) units vertically stacked in series through a charge-generation unit (CGU). The CGU plays an important role for charge generation and injection to the adjacent EL unit in the working process of tandem OLEDs.

Since the electric-field-assisted bipolar charge-generation effect of CGU with the structure of Mg-doped tris(8-hydroxyquinoline) aluminum (Alq_3)/V_2O_5 was demonstrated [4], various CGUs have been reported, such as Li-doped 2,9-dimethyl-4,7-diphenyl-1,10-phenanthroline (BCP)/V_2O_5 [5], Li-doped Alq_3/$FeCl_3$-doped 4,4′-bis-(1-naphthyl-*N*-phenylamino)-biphenyl (NPB) [6], Mg-doped Alq_3/WO_3 [7], Li-doped 4,7-diphenyl-1,10-phenanthroline (Bphen)/MoO_3 [8], Cs_2CO_3-doped BCP/MoO_3 [18], Cs_2CO_3-doped Alq_3/Al/MoO_3 [9], C_{60}/MoO_3-doped NPB [17], CsN_3-doped Bphen/MoO_3 [19], Cs-doped Bphen/tetrafluorotetracyano-quinodimethane(F_4-TCNQ)-doped NPB [10], Mg-doped Alq_3/F_4-TCNQ-doped 4,4′,4″-tris{*N*,-(3-methylphenyl)-*N*-phenylamino}-triphenylamine (MTDATA) [11], fullerene (C_{60})-doped zinc phthalocyanine (ZnPc) [12], etc. Typically, the fabrication of these CGUs requires coevaporation or sputtering processes, which inevitably increases the manufacturing cost of the tandem OLEDs. Besides, the active metals used as an n-type dopant, such as lithium, are known to have high diffusivity in organic layers, and will diminish the device stability [20]. Thus, it is of great interest to investigate the feasibility of developing effective undoped CGUs. Such as Al/WO_3/Au [21], LiF/Al/Au [22], LiF/Ca/Ag [22], LiF/Al/HAT-CN_6 [2], as well as organic semiconductor heterojunctions [23–26], such as copper hexadecafluorophthalocyanine (F_{16}CuPc)/copper phthalocyanine (CuPc) [24], pentacene/C_{60} [25], C_{60}/naphthyl end-capped oligothiophenes [26], etc. However, materials that differ from the material system of the single-unit OLEDs are needed in those reported CGUs, which will increase the complexity of the fabrication process. In this

work, an undoped CGU with the structure of LiF/Al/MoO_3 was studied in tandem OLEDs. The LiF/Al structure was always used as cathode in single-unit OLEDs [27], and MoO_3 was used as a hole-injection layer [28]. Thus, tandem OLEDs with CGU of LiF/Al/MoO_3 did not contain materials that differ from the material system of the single-unit OLEDs, which can render tandem OLEDs processing more feasible.

2 Experimental details In our experiments, all devices were fabricated on patterned ITO-coated glass substrates with a sheet resistance of 20 Ω/□. The ITO glass was cleaned with deionized water and organic solvents, and then exposed to a UV–ozone ambient. All films were fabricated by thermal evaporation. Devices used for operational stability test were encapsulated under a nitrogen atmosphere with epoxy and glass lids. The thickness of the films was determined *in situ* by a quartz-crystal sensor and *ex situ* by a profilometer. The emission area of the device was about 12 mm^2. The detailed process of devices fabrication can be found in our previous reports [29, 30]. Figure 1 exhibits the schematic diagrams of the single-unit OLEDs (device A) and the tandem OLEDs (device B) used in this study. In the tandem OLEDs, just as shown in Fig. 1b, the nondoped structure of LiF/Al/MoO_3 was used as CGU to connect the two identical green emission units consisting of NPB/Alq_3. The luminance–current–voltage (L–I–V) characteristics of the devices were measured using a computer-controlled sourcemeter (Keithley 2602) and a calibrated silicon photodiode. The EL spectra were measured by a PR650 spectrometer. The transmittance was recorded on a Hitachi UV 3010 spectrophotometer. All the measurements were carried out at room temperature under ambient conditions.

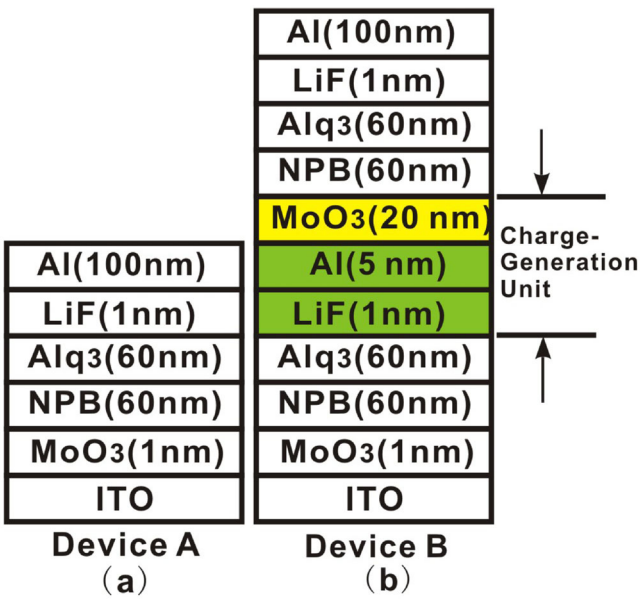

Figure 1 The schematic diagrams of cross-sectional view of the single-unit OLEDs (device A) (a) and the tandem OLEDs (device B) (b) used in this study.

3 Experimental results and discussion The luminance–voltage–current characteristics of single-unit OLEDs (device A) and tandem OLEDs (device B) are shown in Fig. 2a. Because of the larger series resistance of the thicker organic layers in tandem OLEDs, the driving voltage of the tandem OLEDs is higher than that of the single-unit OLEDs at same luminance. For example, at a luminance of 1000 cd m^{-2}, the driving voltage of device A and device B are 7.5 and 18.5 V, respectively. Current efficiency and power efficiency as a function of driving current are shown in Fig. 2b. It can be seen that the current efficiency of tandem OLEDs (device B) using LiF/Al/MoO_3 as CGU is nearly twice that of the single-unit OLEDs (device A). For example, the current efficiency of the tandem OLEDs was about 6.95 cd A^{-1} under the driving current of 650 A m^{-2}, almost 93% improvement over that of the single-unit OLEDs (3.6 cd A^{-1}). As shown in Fig. 2b, the power efficiency of device B reaches about 1.1 lm W^{-1}, which is lower than 1.5 lm W^{-1} of device A because of the higher driving voltage of the tandem OLEDs.

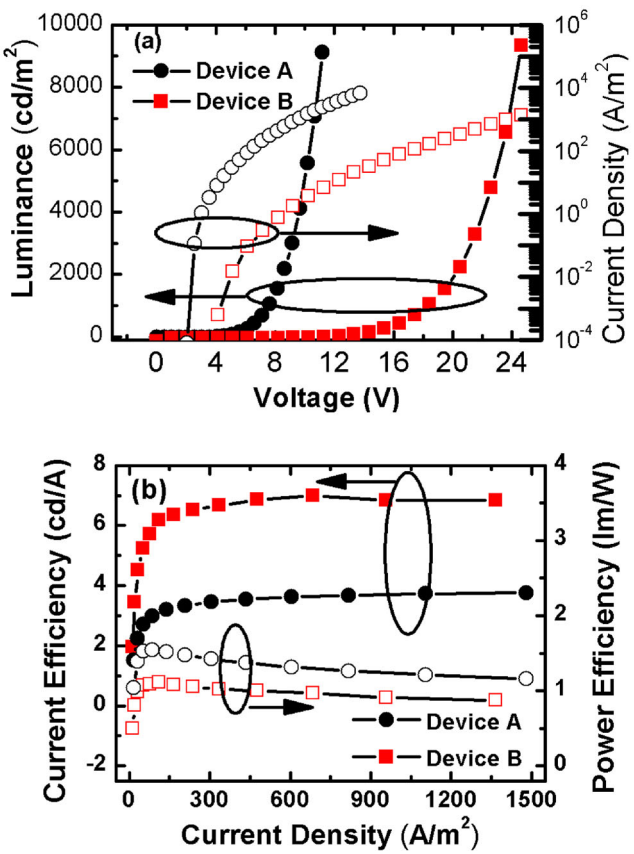

Figure 2 (a) Luminance–voltage–current density characteristics and (b) current efficiency, power efficiency as the function of the driving current (b) for single-unit OLEDs (device A) and tandem OLEDs (device B).

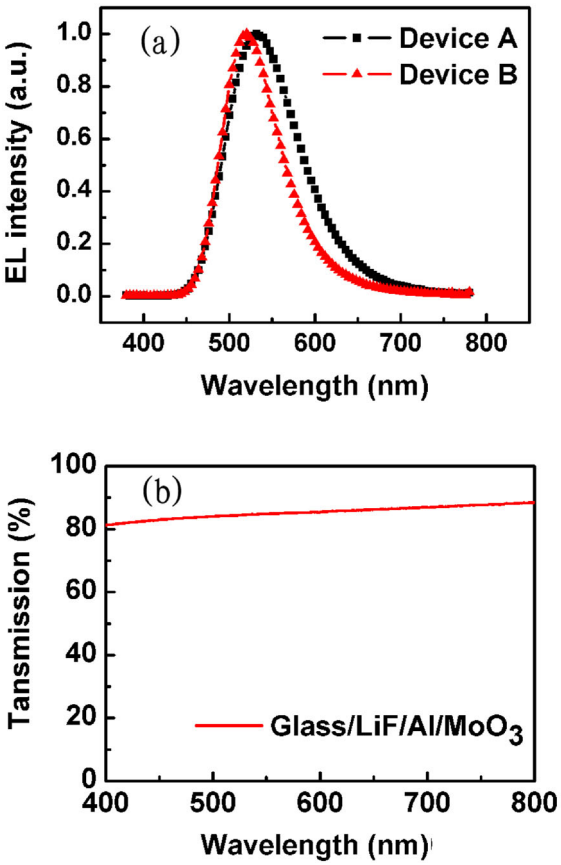

Figure 3 (a) EL spectra of the single-unit OLEDs (device A) and the tandem OLEDs (device B) viewed in the normal direction under driving voltage of 10 V, and (b) transmittance spectra of glass/LiF (1 nm)/Al (5 nm)/MoO_3 (20 nm).

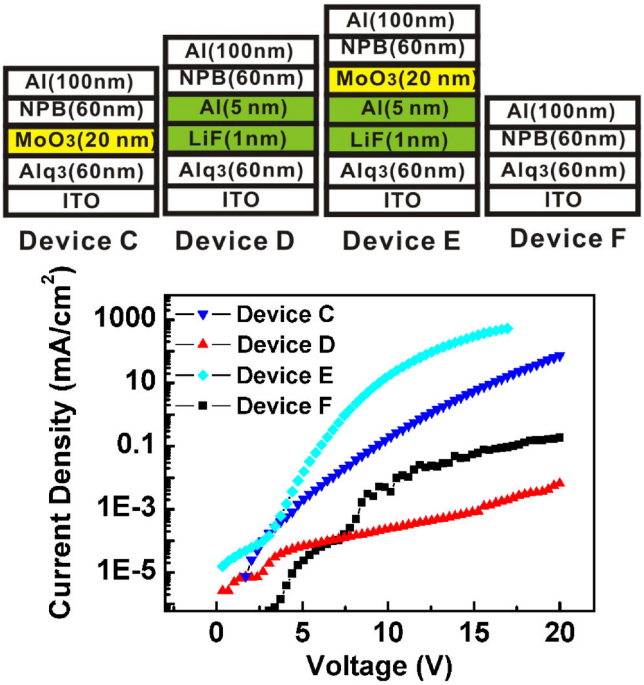

Figure 4 The schematic diagrams of cross-sectional view of device C, device D, device E, and device F, as well as their current–voltage characteristics. Here, ITO was used as the anode, and Al was used as the cathode.

The normalized EL spectra of the single-unit OLEDs (device A) and the tandem OLEDs (device B) are shown in Fig. 3a. All devices emit green light at about 536 nm, but the tandem OLEDs exhibited a narrower spectrum with a full width at half-maximum (FWHM) of 91 nm, while the single-unit OLEDs shows an FWHM of 108 nm. The narrower spectra of device B was ascribed to optical interference between emissions from two stacked emission unit. Figure 3b exhibits the transmittance of the Glass/LiF (1 nm)/Al (5 nm)/MoO_3 (20 nm). It can be seen that the optical transparency of the CGU is larger than 80% over the whole visible spectrum, which indicated that this CGU exhibits potential in the fabrication of white tandem OLEDs.

As shown in Fig. 4, devices with structure of ITO/Alq_3 (60 nm)/interlayer (*X* nm)/NPB (60 nm)/Al (100 nm) were fabricated to investigate the charge-generation mechanism of the CGU. The interlayer are MoO_3 (20 nm), LiF (1 nm)/Al (5 nm), and LiF(1 nm)/Al(5 nm)/MoO_3 (20 nm) for device C, device D, and device E, respectively. Device F with structure of ITO/Alq_3(60 nm)/NPB (60 nm)/Al (100 nm) was also fabricated as a control device. Here, the ITO was used as the anode, and the aluminum as the cathode. The large offset between the Fermi energy of ITO (4.8 eV) and the highest occupied molecular orbital (HOMO) of Alq_3 (5.8 eV), as well as the great offset between the Fermi energy of aluminum (4.3 eV) and the lowest unoccupied molecular orbital (LUMO) of NPB (5.8 eV), served to reduce the external carrier injection. Then, when devices C–F were biased at forward voltage, the current of the device was totally determined by the charge-generation ability of the interlayer. The current–voltage characteristics of devices C–F are shown in Fig. 4. For device C with LiF (1 nm)/Al (5 nm) as interlayer, the lowest current at the same voltage was obtained, which indicated the interlayer consisted of LiF (1 nm)/Al (5 nm) cannot generate charge efficiently. For device D with an interlayer of 20 nm MoO_3, the current was larger than that of the control device (device F), which indicated that the MoO_3 is an efficient CGU. For device E with an interlayer consisting of LiF (1 nm)/Al (5 nm)/MoO_3 (20 nm), the largest current density was achieved at the same voltage. Thus, the MoO_3 plays a critical role of charge generation in this CGU. Recently, the energy level alignment at MoO_3/organic interfaces was determined via UPS and IPES measurements, and the n-type nature, as well as the electron extraction effect of MoO_3 was demonstrated [31, 32]. The charge-generation mechanism of this CGU is shown in Fig. 5. When an external electric field was applied, electrons were extracted from the MoO_3/NPB interface and transported in the MoO_3 layer, while holes were injected into the NPB layer. For the LiF (1 nm)/Al (5 nm) structure, it has

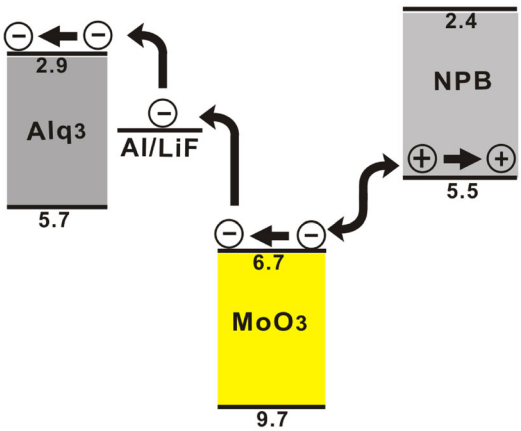

Figure 5 Schematic energy-band diagram of the LiF(1 nm)/Al (3 nm)/MoO_3 (20 nm).

been demonstrated that the Al atoms will react with Alq_3 and molecular LiF, and form an ultrathin n-type doped layer at the Alq_3 surface during the deposition of the Al film [33], which can reduce the electron-injection barrier, as well as enhance the electron injection to the adjacent Alq_3 layer.

The results of operational stability tests for device A (single-unit OLEDs) and device B (tandem OLEDs) are shown in Fig. 6. Tests of those two devices began with the same initial luminance of 3000 cd m^{-2}. The lifetime at 60% of degradation ($t_{0.6}$) of device A was 30 h, whereas the $t_{0.6}$ of device B was 60 h, which was twice that of device A. Because of the higher efficiency, the current density of tandem OLEDs (327 A m^{-2}) is significantly lower than that of the single-unit OLEDs (873 A m^{-2}) at the same initial luminance of 3000 cd m^{-2}, which will reduce the Joule heating in the organic film. Thus, the operational stability for tandem OLEDs was enhanced.

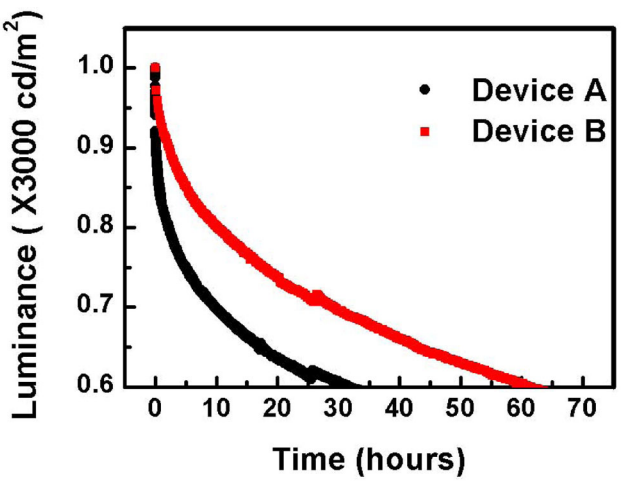

Figure 6 Luminance as a function of the driving time for device A (single-unit OLEDs) and device B (tandem OLEDs) from an initial luminance of 3000 cd m^{-2}, respectively.

4 Conclusions In conclusion, an undoped CGU with the structure of LiF/Al/MoO_3 was demonstrated in tandem OLEDs. Tandem OLEDs with two identical emissive units consisting of NPB/Alq_3 exhibited superior current efficiency over a conventional single-unit device. At 650 A m^{-2}, the current efficiency of the tandem OLEDs was about 6.95 cd A^{-1}, almost doubling that of the single-unit OLEDs. Operational stability of the tandem OLEDs was also enhanced compared with that of the control device. It was demonstrated that MoO_3 acted as a charge-generation layer, in addition the LiF/Al layers acted as an electron-injection unit in this CGU. Furthermore, fabrication of this CGU involves no sputtering or doping process, as well as materials that differ from the material system of the single-unit OLEDs, which will be beneficial for the development of low-cost tandem OLEDs.

Acknowledgements This work was supported by the Basic Research Program of China (2013CB328701-2013CB328706), the National Natural Science Foundation of China (Program No. 61275034), the National Natural Science Young Foundation of Chian (Program No. 61106123), the Natural Science Basic Research Plan in Shaanxi Province of China (Program No. 2012JQ8001), and the Fundamental Research Funds for the Central University (Program No. xjj2012087).

References

[1] C. Yonghua, W. Qi, C. Jiangshan, M. Dongge, Y. Donghang, and W. Lixiang, Org. Electron. **13**(7), 1121–1128 (2012).
[2] T. Chiba, Y. J. Pu, R. Miyazaki, K. Nakayama, H. Sasabe, and J. Kido, Org. Electron. **12**(4), 710–715 (2011).
[3] T. Matsumoto, T. Nakada, J. Endo, K. Mori, N. Kawamura, A. Yokoi, and J. Kido, SID Symp. Digest Tech. Pap. **34**(1), 979–981 (2003).
[4] T. Tsutsui and M. Terai, Appl. Phys. Lett. **84**(3), 440–442 (2004).
[5] F. Guo and D. Ma, Appl. Phys. Lett. **87**(17), 173510 (2005).
[6] L. S. Liao, K. P. Klubek, and C. W. Tang, Appl. Phys. Lett. **84**(2), 167–169 (2004).
[7] C.-C. Chang, J.-F. Chen, S.-W. Hwang, and C. H. Chen, Appl. Phys. Lett. **87**(25), 253501 (2005).
[8] H. Kanno, R. J. Holmes, Y. Sun, S. Kena-Cohen, and S. R. Forrest, Adv. Mater. **18**(3), 339–342 (2006).
[9] C.-W. Chen, Y.-J. Lu, C.-C. Wu, E. H.-E. Wu, C.-W. Chu, and Y. Yang, Appl. Phys. Lett. **87**(24), 241121 (2005).
[10] T.-Y. Cho, C.-L. Lin, and C.-C. Wu, Appl. Phys. Lett. **88**(11), 111106 (2006).
[11] C. W. Law, K. M. Lau, M. K. Fung, M. Y. Chan, F. L. Wong, C. S. Lee, and S. T. Lee, Appl. Phys. Lett. **89**(13), 133511 (2006).
[12] Y. Chen, J. Chen, D. Ma, D. Yan, L. Wang, and F. Zhu, Appl. Phys. Lett. **98**(24), 243309 (2011).
[13] H.-D. Lee, S. J. Lee, K. Y. Lee, B. S. Kim, S. H. Lee, H. D. Bae, and Y. H. Tak, Jpn. J. Appl. Phys. **48**(8), 082101 (2009).
[14] J. X. Tang, M. K. Fung, C. S. Lee, and S. T. Lee, J. Mater. Chem. **20**(13), 2539–2548 (2010).

[15] J.-P. Yang, Q.-Y. Bao, Y. Xiao, Y.-H. Deng, Y.-Q. Li, S.-T. Lee, and J.-X. Tang, Org. Electron. **13**(11), 2243–2249 (2012).
[16] L. Duan, T. Tsuboi, Y. Qiu, Y. Li, and G. Zhang, Opt. Exp. **20**(13), 14564–14572 (2012).
[17] X. Wu, W. Bi, Y. Hua, J. Sun, Z. Xiao, L. Wang, and S. Yin, Appl. Phys. Lett. **102**(24), 243302 (2013).
[18] T. W. Lee, T. Noh, B. K. Choi, M. S. Kim, D. W. Shin, and J. Kido, Appl. Phys. Lett. **92**, (4). 043301 (2008).
[19] K. S. Yook, S. O. Jeon, S. Y. Min, J. Y. Lee, H. J. Yang, T. Noh, S. K. Kang, and T. W. Lee, Adv. Funct. Mater. **20**(11), 1797–1802 (2010).
[20] B. W. D'Andrade, S. R. Forrest, and A. B. Chwang, Appl. Phys. Lett. **83**(19), 3858–3860 (2003).
[21] H. Zhang, Y. Dai, and D. Ma, Appl. Phys. Lett. **91**(12), 123504 (2007).
[22] J. X. Sun, X. L. Zhu, H. J. Peng, M. Wong, and H. S. Kwok, Appl. Phys. Lett. **87**(9), 093504 (2005).
[23] Y. H. Chen and D. G. Ma, J. Mater. Chem. **22**(36), 18718–18734 (2012).
[24] S. L. Lai, M. Y. Chan, M. K. Fung, C. S. Lee, and S. T. Lee, J. Appl. Phys. **101**(1), 014509 (2007).
[25] M. V. M. Rao, T.-S. Huang, Y.-K. Su, and Y.-T. Huang, J. Electrochem. Soc. **157**(1), H69–H71 (2010).
[26] Y. H. Chen, H. K. Tian, Y. H. Geng, J. S. Chen, D. G. Ma, D. H. Yan, and L. X. Wang, J. Mater. Chem. **21**(39), 15332–15336 (2011).
[27] L. S. Hung, C. W. Tang, and M. G. Mason, Appl. Phys. Lett. **70**(2), 152–154 (1997).
[28] H. You, Y. Dai, Z. Zhang, and D. Ma, J. Appl. Phys. **101**(2), 026105 (2007).
[29] B. Jiao, Z. X. Wu, Y. Dai, D. D. Wang, and X. Hou, J. Phys. D: Appl. Phys. **42**, 205108 (2009).
[30] B. Jiao, Z. X. Wu, Q. He, Y. Tian, G. Mao, and X. Hou, J. Phys. D: Appl. Phys. **43**, 035101 (2010).
[31] J. Meyer, S. Hamwi, M. Kroger, W. Kowalsky, T. Riedl, and A. Kahn, Adv. Mater. **24**(40), 5408–5427 (2012).
[32] M. T. Greiner, L. Chai, M. G. Helander, W. M. Tang, and Z. H. Lu, Adv. Funct. Mater. **22**(21), 4557–4568 (2012).
[33] M. G. Mason, C. W. Tang, L. S. Hung, P. Raychaudhuri, J. Madathil, D. J. Giesen, L. Yan, Q. T. Le, Y. Gao, S. T. Lee, L. S. Liao, L. F. Cheng, W. R. Salaneck, D. A. dos Santos, and J. L. Bredas, J. Appl. Phys. **89**(5), 2756–2765 (2001).